EUROPEAN ORGANIZATION FOR NUCLEAR RESEARCH

CERN–PH-EP/2007-008

28 February 2007

Study of multi-muon bundles in cosmic ray showers detected with the DELPHI detector at LEP

DELPHI Collaboration[1]

Abstract

The DELPHI detector at LEP has been used to measure multi-muon bundles originating from cosmic ray interactions with air. The cosmic events were recorded in "parasitic mode" between individual e^+e^- interactions and the total live time of this data taking is equivalent to $1.6 \cdot 10^6$ seconds. The DELPHI apparatus is located about 100 metres underground and the 84 metres rock overburden imposes a cut-off of about 52 GeV/c on muon momenta. The data from the large volume Hadron Calorimeter allowed the muon multiplicity of 54201 events to be reconstructed. The resulting muon multiplicity distribution is compared with the prediction of the Monte Carlo simulation based on CORSIKA/QGSJET01. The model fails to describe the abundance of high multiplicity events. The impact of QGSJET internal parameters on the results is also studied.

PACS 98.70.Sa, 13.85.Tp, 96.40.De
Keywords: Cosmic rays, Cosmic ray interactions, Cosmic ray muons

This paper is dedicated to the memory of Heiner Herr

(Accepted by Astropart. Phys.)

[1]Corresponding author: J. Timmermans, NIKHEF, P.O. Box 41882, 1009 DB Amsterdam, The Netherlands; e-mail: Jan.Timmermans@cern.ch

J.Abdallah[27], P.Abreu[24], W.Adam[56], P.Adzic[13], T.Albrecht[19], R.Alemany-Fernandez[10], T.Allmendinger[19], P.P.Allport[25], U.Amaldi[31], N.Amapane[49], S.Amato[53], E.Anashkin[38], A.Andreazza[30], S.Andringa[24], N.Anjos[24], P.Antilogus[27], W-D.Apel[19], Y.Arnoud[16], S.Ask[28], B.Asman[48], A.Augustinus[10], P.Baillon[10], A.Ballestrero[50], P.Bambade[22], R.Barbier[29], D.Bardin[18], G.J.Barker[58], A.Baroncelli[41], M.Battaglia[10], M.Baubillier[27], K-H.Becks[59], M.Begalli[8], A.Behrmann[59], E.Ben-Haim[22], N.Benekos[34], A.Benvenuti[6], C.Berat[16], M.Berggren[27], D.Bertrand[3], M.Besancon[42], N.Besson[42], D.Bloch[11], M.Blom[33], M.Bluj[57], M.Bonesini[31], M.Boonekamp[42], P.S.L.Booth[†25], G.Borisov[23], O.Botner[54], B.Bouquet[22], T.J.V.Bowcock[25], I.Boyko[18], M.Bracko[45], R.Brenner[54], E.Brodet[37], P.Bruckman[20], J.M.Brunet[9], B.Buschbeck[56], P.Buschmann[59], M.Calvi[31], T.Camporesi[10], V.Canale[40], F.Carena[10], N.Castro[24], F.Cavallo[6], M.Chapkin[44], Ph.Charpentier[10], P.Checchia[38], R.Chierici[10], P.Chliapnikov[44], J.Chudoba[10], S.U.Chung[10], K.Cieslik[20], P.Collins[10], R.Contri[15], G.Cosme[22], F.Cossutti[51], M.J.Costa[55], D.Crennell[39], J.Cuevas[36], J.D'Hondt[3], T.da Silva[53], W.Da Silva[27], G.Della Ricca[51], A.De Angelis[52], W.De Boer[19], C.De Clercq[3], B.De Lotto[52], N.De Maria[49], A.De Min[38], L.de Paula[53], L.Di Ciaccio[40], A.Di Simone[41], K.Doroba[57], J.Drees[59,10], G.Eigen[5], T.Ekelof[54], M.Ellert[54], M.Elsing[10], M.C.Espirito Santo[24], G.Fanourakis[13], D.Fassouliotis[13,4], M.Feindt[19], J.Fernandez[43], A.Ferrer[55], F.Ferro[15], U.Flagmeyer[59], H.Foeth[10], E.Fokitis[34], F.Fulda-Quenzer[22], J.Fuster[55], M.Gandelman[53], C.Garcia[55], Ph.Gavillet[10], E.Gazis[34], R.Gokieli[10,57], B.Golob[45,47], G.Gomez-Ceballos[43], P.Goncalves[24], E.Graziani[41], G.Grosdidier[22], K.Grzelak[57], J.Guy[39], C.Haag[19], A.Hallgren[54], K.Hamacher[59], K.Hamilton[37], S.Haug[35], F.Hauler[19], V.Hedberg[28], M.Hennecke[19], H.Herr[†10], J.Hoffman[57], S-O.Holmgren[48], P.J.Holt[10], M.A.Houlden[25], J.N.Jackson[25], G.Jarlskog[28], P.Jarry[42], D.Jeans[37], E.K.Johansson[48], P.Jonsson[29], C.Joram[10], L.Jungermann[19], F.Kapusta[27], S.Katsanevas[29], E.Katsoufis[34], G.Kernel[45], B.P.Kersevan[45,47], U.Kerzel[19], B.T.King[25], N.J.Kjaer[10], P.Kluit[33], P.Kokkinias[13], C.Kourkoumelis[4], O.Kouznetsov[18], Z.Krumstein[18], M.Kucharczyk[20], J.Lamsa[2], G.Leder[56], F.Ledroit[16], L.Leinonen[48], R.Leitner[32], J.Lemonne[3], V.Lepeltier[22], T.Lesiak[20], W.Liebig[59], D.Liko[56], A.Lipniacka[48], J.H.Lopes[53], J.M.Lopez[36], D.Loukas[13], P.Lutz[42], L.Lyons[37], J.MacNaughton[56], A.Malek[59], S.Maltezos[34], F.Mandl[56], J.Marco[43], R.Marco[43], B.Marechal[53], M.Margoni[38], J-C.Marin[10], C.Mariotti[10], A.Markou[13], C.Martinez-Rivero[43], J.Masik[14], N.Mastroyiannopoulos[13], F.Matorras[43], C.Matteuzzi[31], F.Mazzucato[38], M.Mazzucato[38], R.Mc Nulty[25], C.Meroni[30], E.Migliore[49], W.Mitaroff[56], U.Mjoernmark[28], T.Moa[48], M.Moch[19], K.Moenig[10,12], R.Monge[15], J.Montenegro[33], D.Moraes[53], S.Moreno[24], P.Morettini[15], U.Mueller[59], K.Muenich[59], M.Mulders[33], L.Mundim[8], W.Murray[39], B.Muryn[21], G.Myatt[37], T.Myklebust[35], M.Nassiakou[13], F.Navarria[6], K.Nawrocki[57], R.Nicolaidou[42], M.Nikolenko[18,11], A.Oblakowska-Mucha[21], V.Obraztsov[44], A.Olshevski[18], A.Onofre[24], R.Orava[17], K.Osterberg[17], A.Ouraou[42], A.Oyanguren[55], M.Paganoni[31], S.Paiano[6], J.P.Palacios[25], H.Palka[20], Th.D.Papadopoulou[34], L.Pape[10], C.Parkes[26], F.Parodi[15], U.Parzefall[10], A.Passeri[41], O.Passon[59], L.Peralta[24], V.Perepelitsa[55], A.Perrotta[6], A.Petrolini[15], J.Piedra[43], L.Pieri[41], F.Pierre[42], M.Pimenta[24], E.Piotto[10], T.Podobnik[45,47], V.Poireau[10], M.E.Pol[7], G.Polok[20], V.Pozdniakov[18], N.Pukhaeva[18], A.Pullia[31], J.Rames[14], A.Read[35], P.Rebecchi[10], J.Rehn[19], D.Reid[33], R.Reinhardt[59], P.Renton[37], F.Richard[22], J.Ridky[14], M.Rivero[43], D.Rodriguez[43], A.Romero[49], P.Ronchese[38], P.Roudeau[22], T.Rovelli[6], V.Ruhlmann-Kleider[42], D.Ryabtchikov[44], A.Sadovsky[18], L.Salmi[17], J.Salt[55], C.Sander[19], A.Savoy-Navarro[27], U.Schwickerath[10], R.Sekulin[39], R.C.Shellard[7], M.Siebel[59], A.Sisakian[18], G.Smadja[29], O.Smirnova[28], A.Sokolov[44], A.Sopczak[23], R.Sosnowski[57], T.Spassov[10], M.Stanitzki[19], A.Stocchi[22], J.Strauss[56], B.Stugu[5], M.Szczekowski[57], M.Szeptycka[57], T.Szumlak[21], T.Tabarelli[31], A.C.Taffard[25], F.Tegenfeldt[54], J.Timmermans[33], L.Tkatchev[18], M.Tobin[25], S.Todorovova[14], B.Tome[24], A.Tonazzo[31], P.Tortosa[55], P.Travnicek[14], D.Treille[10], G.Tristram[9], M.Trochimczuk[57], C.Troncon[30], M-L.Turluer[42], I.A.Tyapkin[18], P.Tyapkin[18], S.Tzamarias[13], V.Uvarov[44], G.Valenti[6], P.Van Dam[33], J.Van Eldik[10], N.van Remortel[17], I.Van Vulpen[10], G.Vegni[30], F.Veloso[24], W.Venus[39], P.Verdier[29], V.Verzi[40], D.Vilanova[42], L.Vitale[51], V.Vrba[14], H.Wahlen[59], A.J.Washbrook[25], C.Weiser[19], D.Wicke[10], J.Wickens[3], G.Wilkinson[37], M.Winter[11], M.Witek[20], O.Yushchenko[44], A.Zalewska[20], P.Zalewski[57], D.Zavrtanik[46], V.Zhuravlov[18], N.I.Zimin[18], A.Zintchenko[18], M.Zupan[13]

[2]Department of Physics and Astronomy, Iowa State University, Ames IA 50011-3160, USA
[3]IIHE, ULB-VUB, Pleinlaan 2, B-1050 Brussels, Belgium
[4]Physics Laboratory, University of Athens, Solonos Str. 104, GR-10680 Athens, Greece
[5]Department of Physics, University of Bergen, Allégaten 55, NO-5007 Bergen, Norway
[6]Dipartimento di Fisica, Università di Bologna and INFN, Via Irnerio 46, IT-40126 Bologna, Italy
[7]Centro Brasileiro de Pesquisas Físicas, rua Xavier Sigaud 150, BR-22290 Rio de Janeiro, Brazil
[8]Inst. de Física, Univ. Estadual do Rio de Janeiro, rua São Francisco Xavier 524, Rio de Janeiro, Brazil
[9]Collège de France, Lab. de Physique Corpusculaire, IN2P3-CNRS, FR-75231 Paris Cedex 05, France
[10]CERN, CH-1211 Geneva 23, Switzerland
[11]Institut de Recherches Subatomiques, IN2P3 - CNRS/ULP - BP20, FR-67037 Strasbourg Cedex, France
[12]Now at DESY-Zeuthen, Platanenallee 6, D-15735 Zeuthen, Germany
[13]Institute of Nuclear Physics, N.C.S.R. Demokritos, P.O. Box 60228, GR-15310 Athens, Greece
[14]FZU, Inst. of Phys. of the C.A.S. High Energy Physics Division, Na Slovance 2, CZ-182 21, Praha 8, Czech Republic
[15]Dipartimento di Fisica, Università di Genova and INFN, Via Dodecaneso 33, IT-16146 Genova, Italy
[16]Institut des Sciences Nucléaires, IN2P3-CNRS, Université de Grenoble 1, FR-38026 Grenoble Cedex, France
[17]Helsinki Institute of Physics and Department of Physical Sciences, P.O. Box 64, FIN-00014 University of Helsinki, Finland
[18]Joint Institute for Nuclear Research, Dubna, Head Post Office, P.O. Box 79, RU-101 000 Moscow, Russian Federation
[19]Institut für Experimentelle Kernphysik, Universität Karlsruhe, Postfach 6980, DE-76128 Karlsruhe, Germany
[20]Institute of Nuclear Physics PAN,Ul. Radzikowskiego 152, PL-31142 Krakow, Poland
[21]Faculty of Physics and Nuclear Techniques, University of Mining and Metallurgy, PL-30055 Krakow, Poland
[22]Université de Paris-Sud, Lab. de l'Accélérateur Linéaire, IN2P3-CNRS, Bât. 200, FR-91405 Orsay Cedex, France
[23]School of Physics and Chemistry, University of Lancaster, Lancaster LA1 4YB, UK
[24]LIP, IST, FCUL - Av. Elias Garcia, 14-1^o, PT-1000 Lisboa Codex, Portugal
[25]Department of Physics, University of Liverpool, P.O. Box 147, Liverpool L69 3BX, UK
[26]Dept. of Physics and Astronomy, Kelvin Building, University of Glasgow, Glasgow G12 8QQ
[27]LPNHE, IN2P3-CNRS, Univ. Paris VI et VII, Tour 33 (RdC), 4 place Jussieu, FR-75252 Paris Cedex 05, France
[28]Department of Physics, University of Lund, Sölvegatan 14, SE-223 63 Lund, Sweden
[29]Université Claude Bernard de Lyon, IPNL, IN2P3-CNRS, FR-69622 Villeurbanne Cedex, France
[30]Dipartimento di Fisica, Università di Milano and INFN-MILANO, Via Celoria 16, IT-20133 Milan, Italy
[31]Dipartimento di Fisica, Univ. di Milano-Bicocca and INFN-MILANO, Piazza della Scienza 3, IT-20126 Milan, Italy
[32]IPNP of MFF, Charles Univ., Areal MFF, V Holesovickach 2, CZ-180 00, Praha 8, Czech Republic
[33]NIKHEF, Postbus 41882, NL-1009 DB Amsterdam, The Netherlands
[34]National Technical University, Physics Department, Zografou Campus, GR-15773 Athens, Greece
[35]Physics Department, University of Oslo, Blindern, NO-0316 Oslo, Norway
[36]Dpto. Fisica, Univ. Oviedo, Avda. Calvo Sotelo s/n, ES-33007 Oviedo, Spain
[37]Department of Physics, University of Oxford, Keble Road, Oxford OX1 3RH, UK
[38]Dipartimento di Fisica, Università di Padova and INFN, Via Marzolo 8, IT-35131 Padua, Italy
[39]Rutherford Appleton Laboratory, Chilton, Didcot OX11 OQX, UK
[40]Dipartimento di Fisica, Università di Roma II and INFN, Tor Vergata, IT-00173 Rome, Italy
[41]Dipartimento di Fisica, Università di Roma III and INFN, Via della Vasca Navale 84, IT-00146 Rome, Italy
[42]DAPNIA/Service de Physique des Particules, CEA-Saclay, FR-91191 Gif-sur-Yvette Cedex, France
[43]Instituto de Fisica de Cantabria (CSIC-UC), Avda. los Castros s/n, ES-39006 Santander, Spain
[44]Inst. for High Energy Physics, Serpukov P.O. Box 35, Protvino, (Moscow Region), Russian Federation
[45]J. Stefan Institute, Jamova 39, SI-1000 Ljubljana, Slovenia
[46]Laboratory for Astroparticle Physics, University of Nova Gorica, Kostanjeviska 16a, SI-5000 Nova Gorica, Slovenia
[47]Department of Physics, University of Ljubljana, SI-1000 Ljubljana, Slovenia
[48]Fysikum, Stockholm University, Box 6730, SE-113 85 Stockholm, Sweden
[49]Dipartimento di Fisica Sperimentale, Università di Torino and INFN, Via P. Giuria 1, IT-10125 Turin, Italy
[50]INFN,Sezione di Torino and Dipartimento di Fisica Teorica, Università di Torino, Via Giuria 1, IT-10125 Turin, Italy
[51]Dipartimento di Fisica, Università di Trieste and INFN, Via A. Valerio 2, IT-34127 Trieste, Italy
[52]Istituto di Fisica, Università di Udine and INFN, IT-33100 Udine, Italy
[53]Univ. Federal do Rio de Janeiro, C.P. 68528 Cidade Univ., Ilha do Fundão BR-21945-970 Rio de Janeiro, Brazil
[54]Department of Radiation Sciences, University of Uppsala, P.O. Box 535, SE-751 21 Uppsala, Sweden
[55]IFIC, Valencia-CSIC, and D.F.A.M.N., U. de Valencia, Avda. Dr. Moliner 50, ES-46100 Burjassot (Valencia), Spain
[56]Institut für Hochenergiephysik, Österr. Akad. d. Wissensch., Nikolsdorfergasse 18, AT-1050 Vienna, Austria
[57]Inst. Nuclear Studies and University of Warsaw, Ul. Hoza 69, PL-00681 Warsaw, Poland
[58]Now at University of Warwick, Coventry CV4 7AL, UK
[59]Fachbereich Physik, University of Wuppertal, Postfach 100 127, DE-42097 Wuppertal, Germany
[†] deceased

1 Introduction

The DELPHI (DEtector with Lepton Photon and Hadron Identification) at CERN LEP (Large Electron Positron collider) measured cosmic muons regularly in order to align and calibrate various subdetectors. A major upgrade of the DELPHI hadron calorimeter was completed in 1997. As a result the calorimeter granularity increased substantially and spectacular events like the one shown in Fig. 1 were registered. The trigger studies performed during 1998 have shown that DELPHI can register cosmic events during regular data taking. Whenever there was no triggered e^+e^- interaction, the detector stayed active to record possible cosmic events. In this regime we were able to collect data throughout the years 1999 and 2000.

The experimental hall of DELPHI was located 100 metres underground and the overburden imposed a cut-off of 52 GeV/c on the momenta of vertical muons. This, depending on the particular interaction model, corresponds to a lower limit of primary particle energies of about 10^{14} eV. The upper limit of primary energy, less than 10^{18} eV, follows from the total measurement time of $1.6 \cdot 10^6$ seconds. Although this live time is small compared to standard cosmic ray experiments, the granularity of the detector and the momentum cut-off make the data interesting. The high energy muons originate from meson decays and other processes which take place in the upper atmosphere. They carry information about the first stages of the shower development. Consequently, these data reflect different aspects of the shower than those recorded by experiments on the ground, where the vast majority of detected muons originates from pion decays at low energies.

Reconstruction of cosmic ray interactions at very high energies relies heavily on Monte Carlo (MC) simulations. Hence the interpretation of measured data is dependent on the models of shower propagation, including simulations of high energy hadron collisions, hadron decays and further development of the electromagnetic and hadronic components. While the particle decays and the shower propagation are well described, the most important source of uncertainties originates from models describing the high energy interactions of hadrons at the beginning of shower development. The interaction models such as NEXUS [1], QGSJET [2] or SIBYLL [3] are tuned to available accelerator data at lower energies than those discussed in this paper. The collider experiments are more suited to study phenomena at larger transverse momenta. Thus our data, which can reveal features of particle interactions in the very forward region, are in this sense complementary.

The muon component of cosmic ray showers has been studied with large ground arrays (e.g. [4, 5]) or at large depths corresponding to a momentum cut-off above 1 TeV (e.g. [6–8]). The data at intermediate depths underground are scarce and the experiments detecting muons with a momentum cut-off around 100 GeV/c (e.g. [9]) use less precise detectors than the LEP experiments. Besides DELPHI, similar studies of cosmic rays were performed at ALEPH [10] and L3+C [11]. Detailed model tests [12] show that QGSJET describes best the various correlations between hadronic, electromagnetic and muon components of atmospheric showers in the case of ground experiments. Data registered by underground experiments reflect different shower properties. The aim of this work is to test the interaction model, which sufficiently well describes the ground measurements, using multi-muon data detected underground.

The detector and its overburden are described in Section 2. The conditions of event registration are mentioned in Section 3 and the procedure of event reconstruction is described in Section 4. The chain of programs used to simulate showers is described in

Section 5. The results obtained are given together with predictions of hadronic interaction models in Section 6 and they are discussed in the final Section 7.

2 Detector and its location

DELPHI was a classical collider experiment with numerous subdetectors and a solenoidal magnetic field. A detailed description of the apparatus can be found in [13]. Only a few subdetectors were used for the cosmic muon detection, namely: Time Projection Chamber (TPC), Time Of Flight scintillation detector (TOF), Outer Detector (OD), Barrel part of HAdron calorimeter (HAB) and Barrel MUon chambers (MUB). All these parts were located in the barrel part of the detector (Fig. 2). TOF served to trigger cosmic events.

The HAB detector was a sampling calorimeter and it contained 12000 limited streamer tubes. The iron of the magnet yoke served as an absorber. It consisted of 20 slabs 5 cm thick. Streamer tubes were inserted into the 2 cm wide gaps between individual iron plates. The gas mixture inside the tubes was composed of Ar(10%), CO_2(60%) and isobutane(30%). HAB with its large volume served as the backbone of muon detection. The detection area of HAB was 75 m^2 in the horizontal plane. Each tube in the barrel part of the hadron calorimeter had an effective length of 3.6 m and its cross-section was 1×8 cm^2. All the tubes were parallel to the beam pipe. During the upgrade of the hadron calorimeter in the years 1995 - 1997 each tube was equipped with read-out of its cathode, which consisted of resistive varnish of the whole tube interior [14]. The smallest sensitive cell before the upgrade was about $20 \times 30 \times 35$ cm^3 in (θ, ϕ, R) standard DELPHI coordinate system[1] and the cells were organised in towers pointing to the centre of the detector. After the upgrade the cell size of the cathode readout in the barrel became $360 \times 8 \times 7$ cm^3 [15, 16]. Consequently the granularity in the plane perpendicular to the beams increased about 14 times. Due to technical limitations it was possible to read out signals only on the two outer front-ends of the barrel. The charge deposited on the cathode was integrated for 350 μs and accepted or rejected by a discriminator. Thus in this system of cathode read-out, the signals from individual tubes were either *yes* or *no* and the reconstructed tracks are in fact only projections of the muon trajectories onto the plane perpendicular to the LEP beams, separately for each half of HAB.

The TPC was able to measure the full direction of muon tracks. Due to its relatively small volume it contained only a small fraction of the muons passing through DELPHI (TPC had 10 times smaller detection area compared to HAB). During the standard recording of e^+e^- collisions, the drift time in the TPC is measured from t_0 which is given by the instant of beam cross-over (BCO) inside DELPHI. In the case of cosmic events t_0 was the average arrival time of tracks to the OD.

In extreme cases 50% or more of the tubes in one or both sides of HAB were hit. This led to saturated events where counting of individual muons was not possible anymore. However, the cosmic origin of these events is guaranteed, because in this case vacant tubes appear in parallel lines which follow the direction of the muon bundle and they cannot be caused by any noise in HAB. Moreover, in a few such events the lower bound on the number of muons could be roughly assessed from MUB.

The apparatus was situated about 100 m underground. The surface altitude was 428 m above the sea level. The composition of the rock above the DELPHI experiment is known from a geological survey performed for civil engineering purposes. The simplified picture

[1] as defined e.g. in [13] - R radius, ϕ azimuth angle in plane perpendicular to the beam pipe and θ polar angle (= 0 along beam)

of the overburden structure could be approximated by 5 major geological layers with different mass densities. The density of the rock in the vertical direction varies between 2.2 g/cm^3 and 2.5 g/cm^3 depending on the layer. The total vertical depth of DELPHI location is about 19640 g/cm^2. The resulting energy cut-off for vertical cosmic muons is $\sim$ 52 GeV. The detector was located in a large experimental cavern equipped with three access shafts shown in Fig. 3. This scheme of the experimental area and the overburden was used in simulations.

3 Trigger

The trigger of cosmic events was entirely based on TOF. This detector consisted of a single layer of plastic scintillation counters. Each one was read out by two photomultipliers. The scintillator planks covered the internal side of HAB. Initial attempts to trigger on single muons led to a high trigger rate. Therefore in 1999 the trigger was set up to demand at least 3 active detector sectors to accept an event. It ran in so-called "parasitic mode", i.e. whenever there was no triggered e^+e^- interaction, the trigger stayed sensitive to cosmic events for 4.1 μs after each beam crossing. This short detection window was optimised for e^+e^- interactions.

The beam crossing frequency depended on the number of $e^+(e^-)$ bunches in the collider. During the running mode with 4 bunches in the machine, the beam crossing period was $\sim$ 22.2 μs, while in the 8 bunch mode the period decreased to $\sim$ 11.1 μs. Consequently, the detector was sensitive to cosmic events for 18% of the total data taking time in 4 bunch mode and for 37% in 8 bunch mode. Dedicated cosmic runs (without the beams in the collider) have been performed mainly at the beginning of each year. Although there were no e^+e^- collisions, BCO signals were issued to mimic the 8 bunch mode.

In an ideal case, two muons passing TOF would be sufficient to activate the trigger. In reality the TOF detection efficiency in $Z^0 \rightarrow \mu^+\mu^-$ events was 84%. However, with increasing muon multiplicity the TOF trigger efficiency quickly approaches almost 100%. Already for muon multiplicity $N_\mu = 5$ the TOF efficiency is 99%, for lower multiplicities $N_\mu = 3(4)$ the corresponding efficiencies are 94(97)%. It was found in [17] that with 5 or more muons the trigger stability is assured. Fig. 4 plots the rate of events with muon multiplicity higher than 5 in different run periods. The event rates are consistent within statistical errors and there is no difference between the runs with and without beams in LEP. In total, taking into account various bunch schemes and the 4.1 μs detection window, the accumulated effective live time is $T_{eff} = 1.6 \cdot 10^6$ s (= 18.5 days).

4 Event reconstruction

The tracks of cosmic muons were reconstructed from hadron calorimeter data by the ECTANA program [18], which scans signals in the HAB modules and finds track patterns of hit streamer tubes. This package has the advantage that it was developed not only for studies of e^+e^- collisions, i.e. tracks coming from the interaction point in the centre of the detector, but it has the option for cosmic events as well. When running in cosmic mode it allows tracks originating anywhere in the calorimeter to be reconstructed without an explicit cut on the track impact parameter. The search for active streamer tubes starts from the outer planes of a given module and continues inwards. A group of at least 4 aligned hits is taken as a track element. The track element is also required to have a reasonable density of hits, at least 30% of tubes along its length have to be active. All possible hypotheses starting from a certain hit found during the scan are analysed, and the positions of hits are fitted by a straight line. The best fit in terms of the number of hits and χ^2 is stored. Before accepting the track, its similarity with other hypotheses was checked to avoid double counting.

The length of the reconstructed track was required to be larger than 50 cm. It was possible to fit radii of curvature of the bent tracks, however, there were only a few such tracks and their radii were quite large. Therefore the coordinates of active tubes were fitted only by straight lines in the final analysis. The matching between track elements from different calorimeter sectors was performed. The number of reconstructed tracks was considered as the reconstructed multiplicity of an event. The performance and functionality of the ECTANA program were checked with MC studies that compared parameters of reconstructed and injected events. However, no MC tuning of the reconstruction software was needed.

The analysed data sample consists of 54201 events with muon multiplicities bigger than 3. They were registered during the years 1999 and 2000. The number of events with multiplicity above a given value is given in Tab. 1 and the differential multiplicity distribution is shown in Fig. 5.

Altogether there were only 7 saturated events like the one depicted in Fig. 6 where more then 50% of the tubes were hit. In the case of saturated events vacant tubes make parallel line patterns which cannot result from a glitch of the electronics. The saturated events are expected to have multiplicity higher than the highest multiplicity reconstructed from unsaturated events ($N_\mu > 127$). Moreover, in two of these events we were able to assess the lower limit of the multiplicity from the proportionality between the number of MUB anode hits and reconstructed muon multiplicity from HAB (Fig. 7). However, this procedure was not possible in all events. The MUB time window is only 5.9 μs after BCO and the events coming at the end of trigger time window 4.1 μs after BCO are not registered properly as the necessary drift time is 2.5 μs.

In general, the muon tracks inside bundles are almost parallel as demonstrated in Fig. 8. In this picture we plot the angle α between the vertical direction and the track projection onto the plane perpendicular to the LEP beams. The track collinearity helped to find high multiplicity events originating from muon interactions close to the detector. The manual scanning was done on all events with $N_\mu > 30$. Altogether we have rejected 14 events with diverse directions of tracks. They correspond to 1.3% of the 1065 scanned events. The parallelism of reconstructed tracks was checked also by the cut that requires more than 50% of reconstructed tracks to be aligned within 5° of the mean value of all track angles in the event. This cut rejected the same events as the scanning procedure.

As already mentioned above, the cathode read-out could not detect how many muons hit one single tube. Therefore at higher multiplicities muons start to shadow each other and the reconstructed multiplicity is in fact a lower limit of the real event multiplicity. However, even the highest reconstructed multiplicities around 120 are still strongly correlated with the initial multiplicity as can be seen from Fig. 9, where the reconstructed multiplicity in MC data is plotted as a function of the number of muons injected into HAB.

Unlike the hadron calorimeter, the TPC gives full spatial information on traversing muons. The drawback is its relatively small size. The track reconstruction from the TPC was possible with standard DELPHI software tools with the provision for start of the drift time (see Section 2). Due to the disproportion of TPC and HAB sizes, the respective multiplicities do not correlate well. However, we were able to reconstruct the muon bundle directions from the TPC and to compare the multiplicities from the TPC with MC predictions [17].

5 Simulation

To simulate the response of DELPHI to cosmic-ray induced showers, we have set up a chain of simulation programs. The high energy interactions were modelled by the QGSJET01 [2] program implemented within the CORSIKA [19] package[2] . The rock above the DELPHI detector and the shape of the experimental cavern as well as the basic structures such as concrete walls and the three access shafts were represented according to Fig. 3 and simulated by GEANT3 [20]. Full simulation of the detector response was provided by the DELSIM [21] simulation package.

As the chemical composition of cosmic rays is not well known, we have used only two limiting cases of hadron primary particles - protons and iron nuclei. Data sets were generated for both types of primary particles in 12 energy intervals 10^{12} - $3{\cdot}10^{12}$ eV, $3{\cdot}10^{12}$ - 10^{13} eV, etc. up to $3{\cdot}10^{17}$ - 10^{18} eV. The lowest energy interval barely contributes due to the muon energy cut-off of 52 GeV and the condition $N_\mu > 3$. Also the highest energy interval contributes very little, if at all, because of the relatively short observation time. The lower energy limit depends on the interaction model and on the thickness of the overburden while the upper limit is given by the flux value used for normalisation and the observation time. As these two limits are not given reliably we have used a wider energy range for the simulations.

All CORSIKA simulations were done without "thinning". At high energies ($E > 10^{17}$ eV) the thinning option speeds up simulations of showers with billions of secondary particles by discarding a defined fraction of the secondaries and by ascribing the remaining particles certain weights. However, this option might introduce additional systematic errors. For this reason full event simulation was used in the analysis.

The data samples were generated according to an energy dependence $\sim E^{-\gamma}$ using the spectral index $\gamma = 1$ in order to obtain sufficient representation of events at the upper part of the energy spectrum. Events were then re-weighted according to one of the assumed energy spectra (see below).

Shower centres were smeared uniformly over a circular area with radius $R = 200$ m around the DELPHI detector. This radius value was chosen as optimal because smaller R values led to an increased fraction of lost events with small muon multiplicities while larger radii would imply the necessity of using large data samples to produce enough events with high muon multiplicities. This is demonstrated in Fig. 10 which shows the stability of the simulated multiplicity distribution as a function of R. For each radius the ratio of occupancies in two adjacent bins in the final integral multiplicity[3] distribution is plotted. With increasing values of R, the simulated multiplicity distribution stabilises. At $R = 200$ m the stability is reached at all simulated energies. Furthermore, the radius of 200 m ensures that the fraction of lost events at the lowest multiplicity $N_\mu = 4$ is smaller than 0.5%.

During the smearing of showers with $E < 10^{16}$ eV each shower was used 10 times. For higher energies the number of moves is 100. Taking 100 moves at energy $> 10^{16}$ eV, one CORSIKA generated shower contributed to the simulated spectrum at $N_\mu > 45$ on

[2] First analyses with QGSJET model were performed with CORSIKA *ver. 6.014* from March 2002. Later studies of QGSJET with modified parameters used CORSIKA *ver. 6.031* from February 2004. It was checked that the results of the two simulations were independent of the CORSIKA version.

[3] Defined in Section 6.

average only once. Since the events with $N_\mu > 45$ are dominated by primary energies higher than 10^{16} eV, the relatively high number of moves is, in fact, chosen optimally.

The generated data set at $N_\mu > 45$ (which corresponds roughly to $E \sim 10^{16}$ eV) was about 20 times larger than the real data sample. At lower multiplicities (i.e. lower energies) the samples were about equal. The stability of the results was also checked by doubling the size of the MC data sets.

The normalisation of the simulated multiplicity distributions depends necessarily on the assumed energy spectrum of primary particles. Four spectra corresponding to different lines in Fig. 11 were assumed. Lines *1, 2* and *3* all represent power law indices $\gamma = 2.7$ below the knee ($E_{\mathrm{knee}} = 3 \cdot 10^{15}$ eV) and $\gamma = 3.0$ above the knee, thus they have the same shape of energy dependence and they differ by the total flux only. Assumption *1b* is defined by exponents $\gamma = 2.6$ below and $\gamma = 3.05$ above the knee. These spectral indices were used for tests of QGSJET01 with changed internal parameters.

The most notable contributions to the systematic errors are our imperfect knowledge of the overburden and due to a hardware effect which in certain situations caused cross-talk of the cathode read-out and appeared as a wider muon track that can shadow more muons than the normal track. The effect of inaccurate knowledge of the overburden was taken into account by changing the rock density by $\pm5\%$ in all geological layers. Changes of multiplicity distribution induced by this density variations stay within 5%. The cross-talk has been studied in detail in $Z^0 \to \mu^+\mu^-$ interactions. Based on this it was incorporated into the MC. The systematic error induced by this effect was checked in MC by using two options: one with full cross-talk simulation taken into account and another with this simulation switched off. It was found that the impact of cross-talk on the final multiplicity distribution is less than 5% of the number of events at high multiplicities. The upper bound of the possible live time error was estimated using the knowledge of the DELPHI dead time and it is about 2%. Due to the DELPHI magnetic field, another effect which might induce systematic error is the possible track matching inefficiency in the upper and the lower part of HAB for low energy muons. Assuming only straight lines in track reconstruction we could double count curved tracks. The effect was studied using the option of the ECTANA package that enabled to search also for curved tracks. It was found that the maximal impact on the final multiplicity distribution decreases with increasing multiplicity and it is about 8% for multiplicities below 15, 4% at integrated multiplicities larger than 20, 3% for multiplicities larger than 45 and 2% for multiplicities larger than 70.

The overall systematic error is $\lesssim 8\%$ at high multiplicities ($N_\mu \geq 45$) which is below the statistical uncertainty. More detailed discussion of the whole simulation is provided in [17].

6 Results

6.1 Directions of muon bundles

The most straightforward and MC-independent results are those concerning the directions of muon bundles. As explained already above, it was possible to reconstruct the full spatial direction of the tracks only from TPC data. As the TPC reconstruction depends on the mean arrival time to OD, we have selected higher multiplicity events with more than 15 muons in HAB and at least 4 reconstructed tracks in TPC. This cut corresponds to primary energies of about $\sim 10^{15}$ eV. The sky plot of event directions in galactic coordinates is shown in Fig. 12. The event direction is given as a mean direction of individual muons and the pointing precision is a few degrees due to multiple scattering in the overburden, detector precision and unknown core position of the shower. There is no apparent clustering of events.

The absence of point sources is demonstrated also by the dependence of the event rate on sidereal time. Fig. 13 shows no significant modulation of the rate during the sidereal day. The small dip disappears at higher multiplicities.

The lack of point like anisotropies in the data justifies the assumption of uniform distribution of cosmic ray directions which is used in MC simulations.

6.2 Muon multiplicities

The shadowing effect reduces the number of reconstructed tracks when compared to the number of muons entering the calorimeter. In fact we measure only a lower limit of the event multiplicity and therefore we plot the integrated multiplicity distributions where all events with given multiplicity or higher contribute to the corresponding bin. The measured distribution is plotted in Fig. 14a together with MC simulations of proton and iron induced showers.

Taking into account that the composition of primary cosmic rays is light at energies $\sim 10^{14}$ eV the data should follow the MC prediction for proton primary particles at small multiplicities. This behaviour is guaranteed only by flux value *1* from Fig. 11. However, this value represents the upper limit of measured fluxes. Taking into account the spread of flux *1* - *3*, we obtain for the MC prediction the bands demonstrated in Fig. 14b.

Evidently even the highest flux value combined with the assumption of pure iron primaries is not sufficient to describe the surplus of high multiplicity events. The excess of events in the region $N_\mu \geq 80$ is 1.9 σ (based on statistical errors) for flux *1*; assuming a more realistic flux value *2*, the discrepancy reaches about 3 σ. One is tempted to interpret Fig. 14 as a convolution of proton and iron induced showers. However, this would mean that the primary particles at lower energies would be only protons while at the higher energies the primaries would be entirely iron nuclei. The contributions of individual energy bins in the case of iron primaries are detailed in Fig. 15. Fig. 16 shows the distribution of projected angle α measured in HAB as compared to MC event samples with $N_\mu \geq 4$ and $N_\mu \geq 20$ respectively. The lower multiplicity corresponds to the point in Fig. 14 where data can be described by proton primaries. The second multiplicity interval represents the region where MC simulation of iron nuclei best describes the data.

The saturated events appear in the simulation in the same way as in the data as events with more than 50% of the tubes hit. In the case of primary protons and flux *1* the number of MC saturated events is 1.1 $\pm$ 0.4. In the case of iron primaries the total number of expected saturated events is 3.3 $\pm$ 1.1 compared to 7 saturated events in the real data.

Although we have tested only the QGSJET model, it is clear that the use of other models would lead to an even greater discrepancy as QGSJET predicts higher muon densities close to the shower core than other models do (e.g. SIBYLL or DPMJET [24]). Because of this, it was suggested [25] to test the sensitivity of the produced multiplicity spectra to QGSJET internal parameters. In [26] a set of QGSJET01 parameters is modified; namely the inelastic cross-section of *p*-*p* (*p*-*N*) is reduced and the elasticity of the collisions is increased. It is argued that such modifications can improve consistency between measurements of cosmic ray composition by experiments based on shower arrays and by Cerenkov or fluorescence telescopes. Reference [26] suggests several possible modifications. In the following we will keep its notation and denote the tested model as modification *3a*. The result obtained with the modified QGSJET is compared with the data and with the original QGSJET01 in Fig. 17a.

The model *3a* enlarges the region where the data are between the predictions for proton and iron induced showers. In the case of unmodified QGSJET01, the data reach the iron curve at multiplicity $\sim$ 20. Using *3a*, the data are consistent with a mixture of light and heavy components up to a multiplicity $\sim$ 70. The slight event excess in data is still apparent at the highest multiplicities, however, now with somewhat smaller significance.

The number of events at low muon multiplicities in the case of proton primaries and model *3a* (Fig. 17a) is now larger than in the data. The smaller and more realistic flux *1b* predicts a number of low multiplicity events consistent with the data as seen from Fig. 17b. At high multiplicities the model *3a* predicts of course less events with flux *1b* than with flux assumption *1*. However, the prediction of model *3a* with spectrum *1b* is still above the prediction of QGSJET with flux *1*.

7 Conclusions

The fine granularity hadron calorimeter of the DELPHI experiment was used to measure multi-muon events originating from cosmic ray showers. The multiplicity distribution of muon bundles cannot be described by current Monte Carlo models in a satisfactory way. It is difficult to express the disagreement quantitatively as we have to use flux values measured elsewhere and also the chemical composition of initial particles is not well known. However, even the combination of extreme assumptions of highest measured flux value and pure iron spectrum fails to describe the abundance of high multiplicity events. Similar qualitative conclusions can be drawn from measurements of ALEPH [10] and L3+C [27], where muon bundles (up to multiplicity of about $\sim$ 30) were studied in coincidence with the ground array signals.

The tested QGSJET-based model with modified cross-sections [26] performs somewhat better but it uses a value of the *p*-*p* total cross-section at the lowest limit allowed by CDF [28], E710 [29] and E811 [30] measurements. Justification of this assumption can be given only by future experiments. Hadron interactions at energies beyond the reach of accelerators are not very well known. Recently, also a more exotic explanation [31], based on the assumption of the presence of strangelets in cosmic rays, has been suggested to describe enhanced production of high multiplicity multi-muon events.

The main conclusion is that the multi-muon data from cosmic ray showers detected at intermediate depths are quite sensitive to the dynamics of initial high energy interactions. In our case the primary collisions leading to high multiplicity events ($N_\mu > 45$) correspond to interactions at energies equivalent to about 5 TeV in the *pp* centre-of-mass system. This energy region has been so far inaccessible to laboratory measurements. However, even after LHC data become available, muon underground measurements have the potential to reveal some details of interactions in the very forward direction which are inaccessible to collider experiments. Thus they are important for the tuning of high energy interaction models which are indispensable for measurements and energy reconstruction of cosmic rays at even higher energies of the order 10^{20} eV, inaccessible to present and near future accelerators.

Acknowledgements

We are greatly indebted to our technical collaborators and to the funding agencies for their support in building and operating the DELPHI detector.

We acknowledge in particular the support of
Austrian Federal Ministry of Education, Science and Culture, GZ 616.364/2-III/2a/98,
FNRS–FWO, Flanders Institute to encourage scientific and technological research in the industry (IWT) and Belgian Federal Office for Scientific, Technical and Cultural affairs (OSTC), Belgium,
FINEP, CNPq, CAPES, FUJB and FAPERJ, Brazil,
Ministry of Education of the Czech Republic, project LC527,
Academy of Sciences of the Czech Republic, project AV0Z10100502,
Grant Agency of the Czech Republic GACR, 202/06/P006,
Commission of the European Communities (DG XII),
Direction des Sciences de la Matière, CEA, France,
Bundesministerium für Bildung, Wissenschaft, Forschung und Technologie, Germany,
General Secretariat for Research and Technology, Greece,
National Science Foundation (NWO) and Foundation for Research on Matter (FOM), The Netherlands,
Norwegian Research Council,
State Committee for Scientific Research, Poland, SPUB-M/CERN/PO3/DZ296/2000, SPUB-M/CERN/PO3/DZ297/2000, 2P03B 104 19 and 2P03B 69 23(2002-2004)
FCT - Fundação para a Ciência e Tecnologia, Portugal,
Vedecka grantova agentura MS SR, Slovakia, Nr. 95/5195/134,
Ministry of Science and Technology of the Republic of Slovenia,
CICYT, Spain, AEN99-0950 and AEN99-0761,
The Swedish Research Council,
Particle Physics and Astronomy Research Council, UK,
Department of Energy, USA, DE-FG02-01ER41155.

References

[1] H. J. Drescher *et al.*, Phys. Rep. **350** (2001) 93.
[2] N. N. Kalmykov *et al.*, Nucl. Phys. Proc. Suppl. **52B** (Issue 3) (1997) 17.
[3] R. S. Fletcher *et al.*, Phys. Rev. D **50** (1994) 5710.
[4] T. Antoni *et al.* [KASCADE Collaboration], Astropart. Phys. **16** (2002) 373.
[5] K. G. Gibbs *et al.* [CASA Collaboration], Nucl. Instr. Meth. A **264** (1988) 67.
[6] Ch. Berger *et al.* [FREJUS Collaboration], Phys. Rev. D **40** (1989) 2163.
Ch. Berger *et al.* [FREJUS Collaboration], Z. Phys. C **48** (1990) 221.
[7] H. Adarkar *et al.*, Phys. Lett. B **267** (1991) 138.
[8] M. Aglietta *et al.* [MACRO and EAS-TOP Collaboration], Astropart. Phys. **20** (2004) 641.
[9] Yu. M. Andreyev *et al.*, in *Proceedings of the 21st Cosmic Ray Conference*, Adelaide, Australia, 1990, Vol. 9, p. 301.
[10] V. Avati *et al.*, Astropart. Phys. **19** (2003) 513.
[11] O. Adriani *et al.* [L3 Collaboration], Nucl. Instr. Meth. A **488** (2002) 209.
[12] T. Antoni *et al.* [KASCADE Collaboration], J. Phys. G **25** (1999) 2161.
[13] P. Aarnio *et al.* [DELPHI Collaboration], Nucl. Instr. Meth. A **303** (1991) 233.

[14] P. Abreu *et al.* [DELPHI Collaboration], Nucl. Instr. Meth. A **378** (1996) 57.
[15] I. Azinenko *et al.*, IEEE Trans. on Nucl. Science **NS-42** No.4 (1995) 485.
[16] I. Azinenko *et al.*, IEEE Trans. on Nucl. Science **NS-43** No.3. (1996) 1751.
[17] P. Travnicek, PhD. thesis, Charles University, Prague 2004, CERN-THESIS-2006-032 also available at: www-hep2.fzu.cz/∼travnick/thesis.ps.gz.
[18] J. Ridky, V. Vrba, J. Chudoba, DELPHI NOTE 99-181 TRACK 96, (1999).
[19] D. Heck *et al.*, FZKA-6019, (1998), Forschungszentrum Karlsruhe.
[20] R. Brun *et al.*, GEANT3, *Report CERN DD/EE/84-1* (1984), CERN, Geneva.
[21] DELPHI Collaboration, DELPHI NOTE: 89-67 PROG 142, (1989).
[22] K. Hagiwara *et al.* [Particle Data Group], Phys. Lett. B **592** (2004) 1.
[23] M. A. Lawrence *et al.*, J. Phys. G **17** (1991) 733.
[24] J. Ranft, Phys. Rev. D **51** (1995) 64.
[25] Ralph Engel and Jörg Hörandel, private communication.
[26] J. R. Hörandel, J. Phys. G **29** (2003) 2439.
[27] H. Wilkens [L3 Collaboration], *Proceedings of the 28th Cosmic Ray Conference*, Tsukuba 2003, Cosmic Ray 1131-1134.
[28] F. Abe *et al.* [CDF Collaboration], Phys. Rev. D **50** (1994) 5550.
[29] N. A. Amos *et al.* [E710 Collaboration], Phys. Lett. B **243** (1990) 158.
[30] C. Avila *et al.* [E811 Collaboration], Phys. Lett. B **445** (1999) 419.
[31] M. Rybczynski, Z. Wlodarczyk and G. Wilk, Acta Phys. Polon. B **33** (2002) 277.

	number of events
$N_\mu > 3$	54201
$N_\mu \geq 30$	1065
$N_\mu \geq 70$	78
$N_\mu \geq 100$	24

Table 1: Multiplicities of reconstructed events.

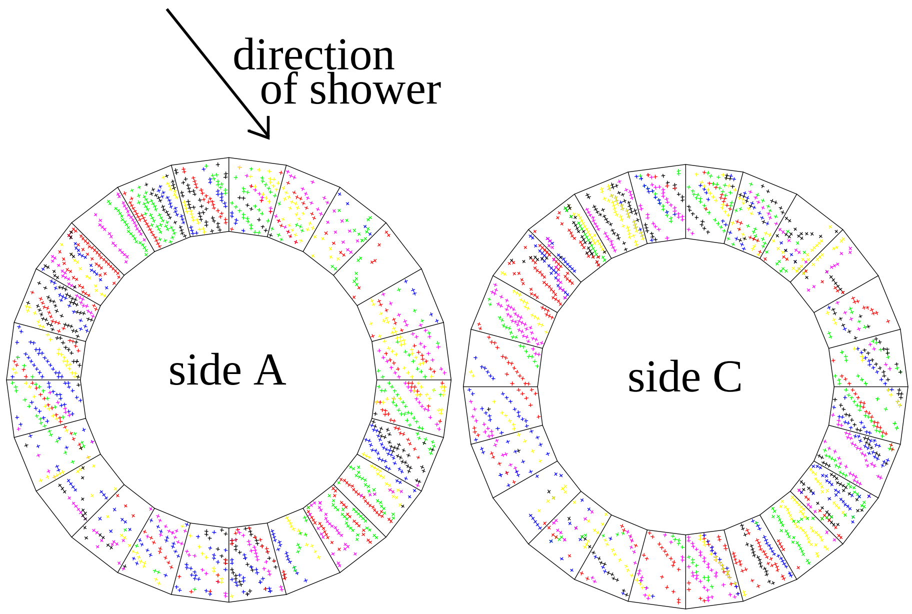

Figure 1: High multiplicity cosmic event as seen by hadron calorimeter. The number of reconstructed tracks was 127.

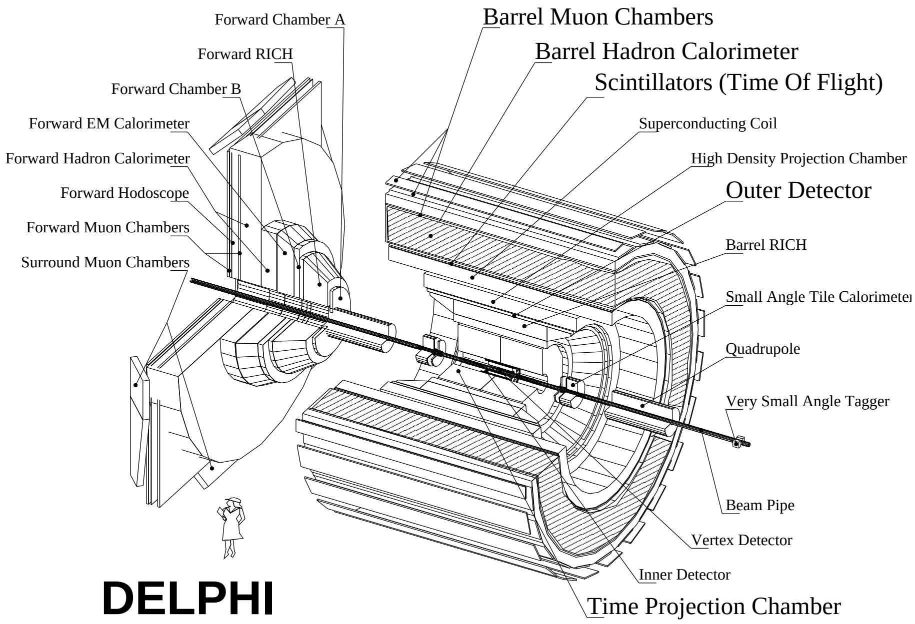

Figure 2: The layout of the DELPHI detector; the hatched area represents the hadron calorimeter. Subdetectors used in this work are marked by larger letters.

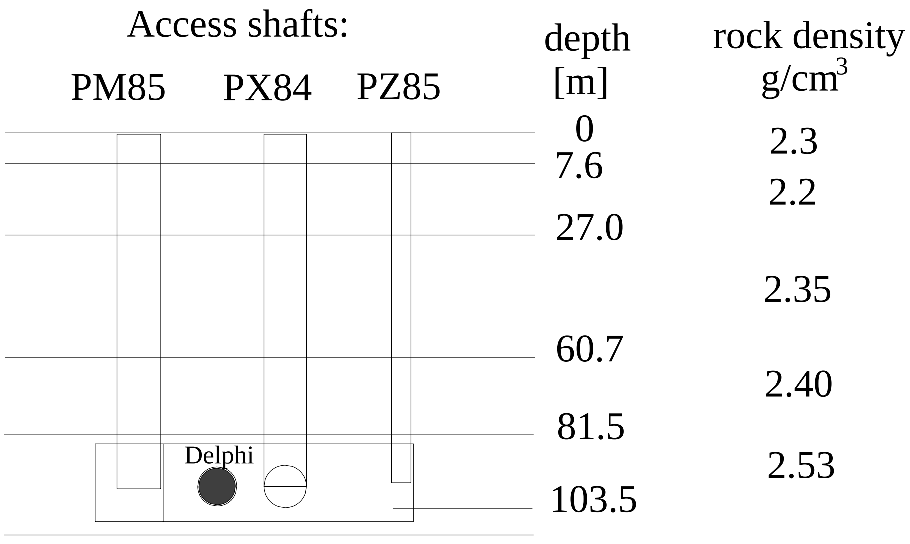

Figure 3: Schematic picture of rock overburden above DELPHI detector.

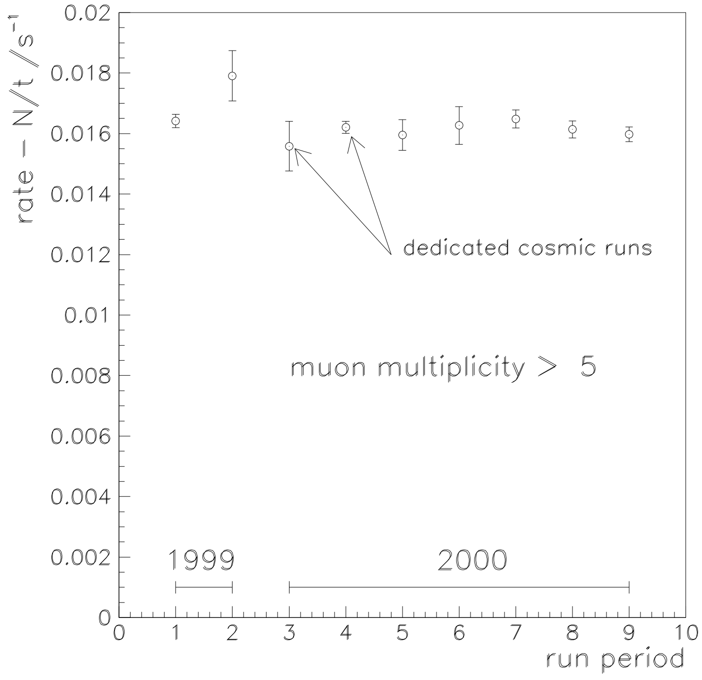

Figure 4: Event rates ($N_\mu > 5$) for different run periods.

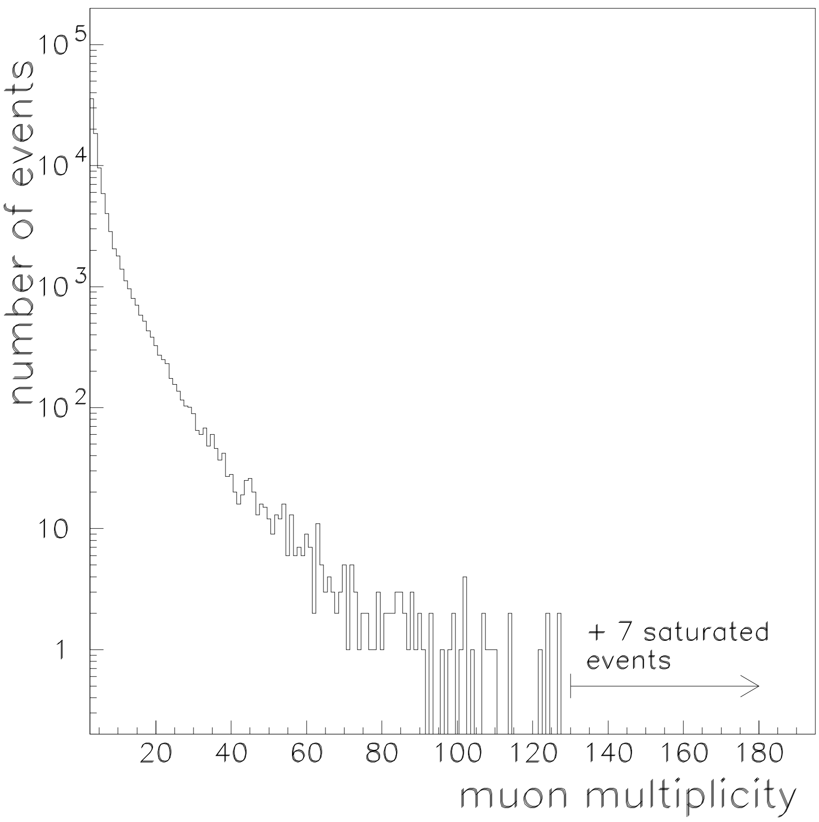

Figure 5: Differential muon multiplicity distribution.

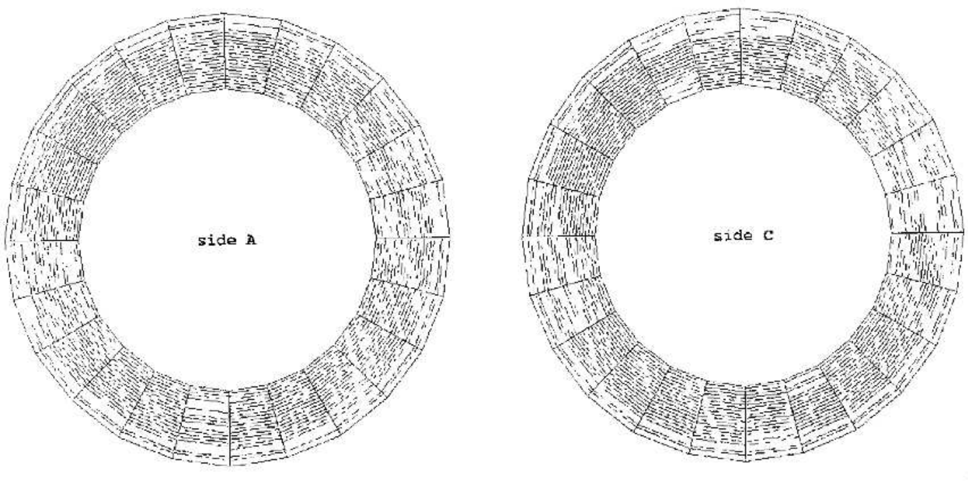

Figure 6: A saturated event in the hadron calorimeter. Vacant tubes show voids in the muon bundle.

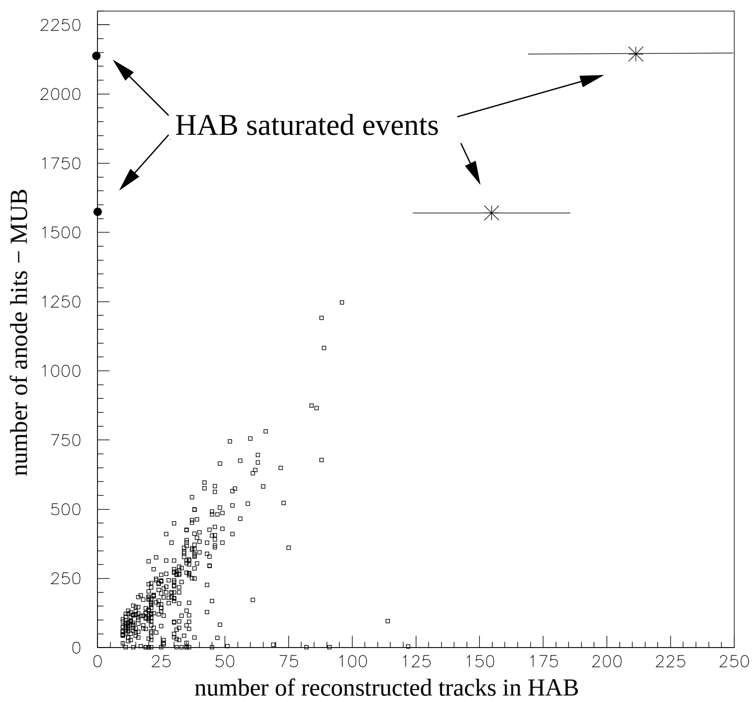

Figure 7: Multiplicity reconstruction of saturated events from MUB data.

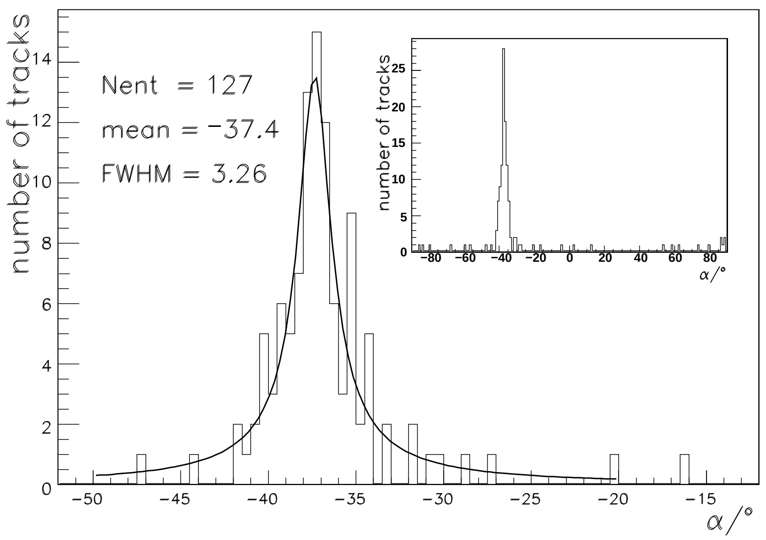

Figure 8: Projected angle distribution in a high multiplicity event.

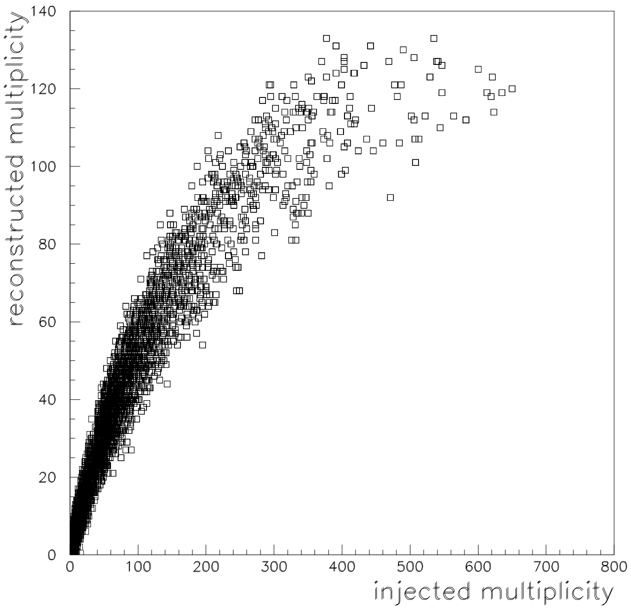

Figure 9: The correlation between injected and reconstructed numbers of muons in MC simulation.

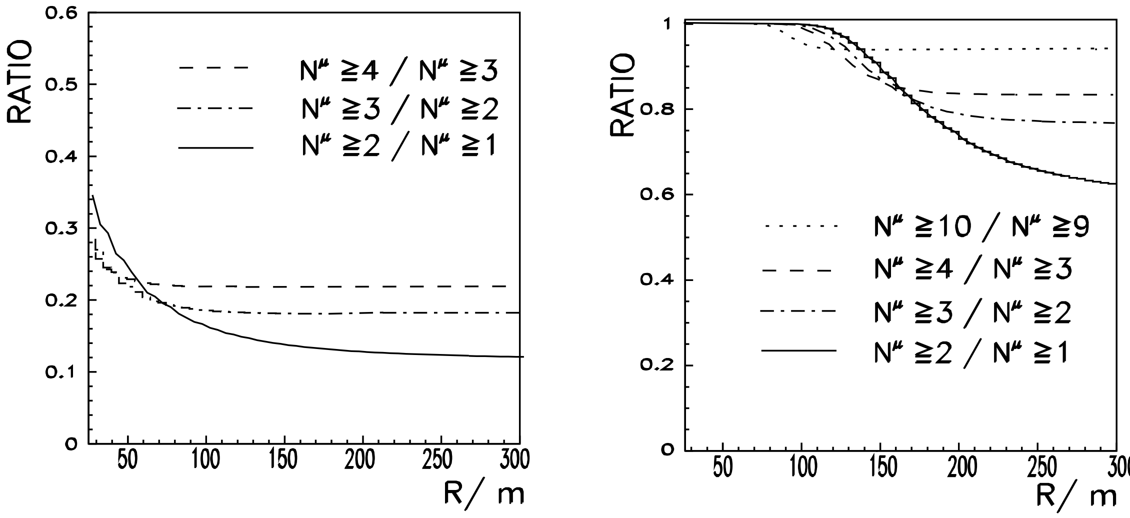

a) b)

Figure 10: Ratio of two adjacent bins (see legends inside the plots) of integral multiplicity distribution as a function of the parameter R. The plots correspond to iron induced vertical showers at a primary energy of 10^{14} eV (a) and 10^{17} eV (b).

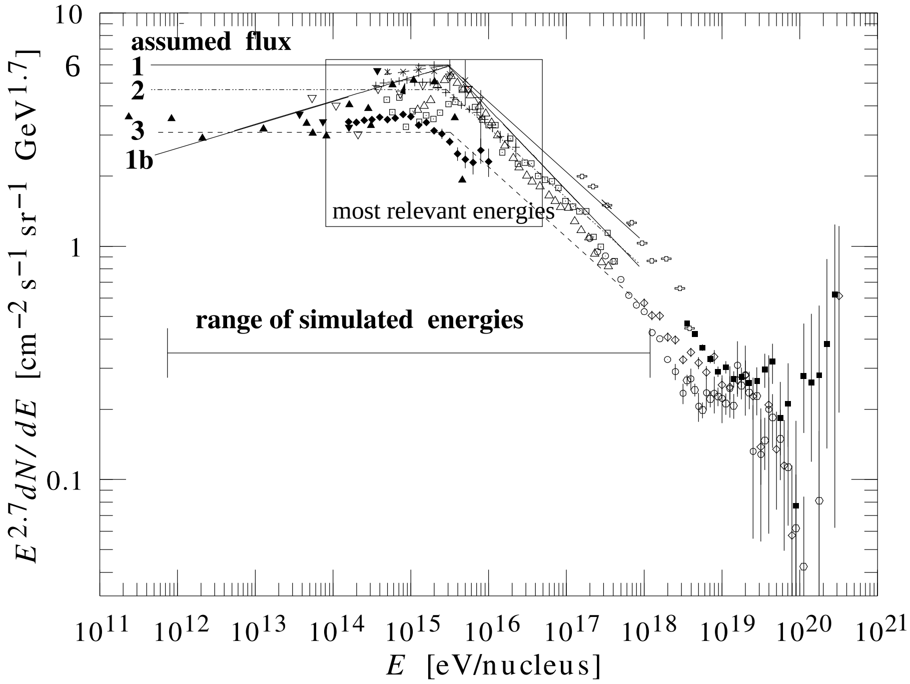

Figure 11: Assumed fluxes compared to various measurements. The picture is taken from [22] and modified. The squares close to line *1* correspond to results of Haverah Park taken from [23]. The data points were added using the macro available at http://astroparticle.uchicago.edu/announce.html. Fluxes are multiplied by $E^{2.7}$.

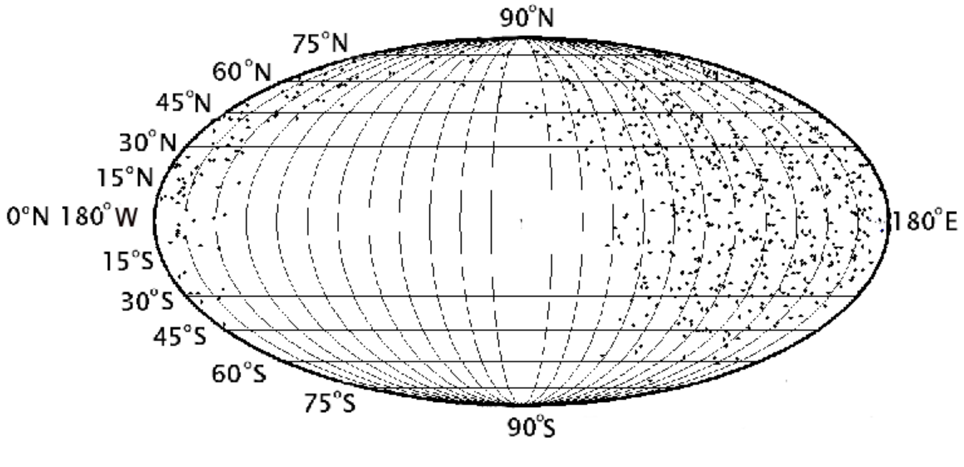

Figure 12: Galactic coordinates of events with more than 15 tracks in HAB and more than 3 reconstructed tracks in TPC.

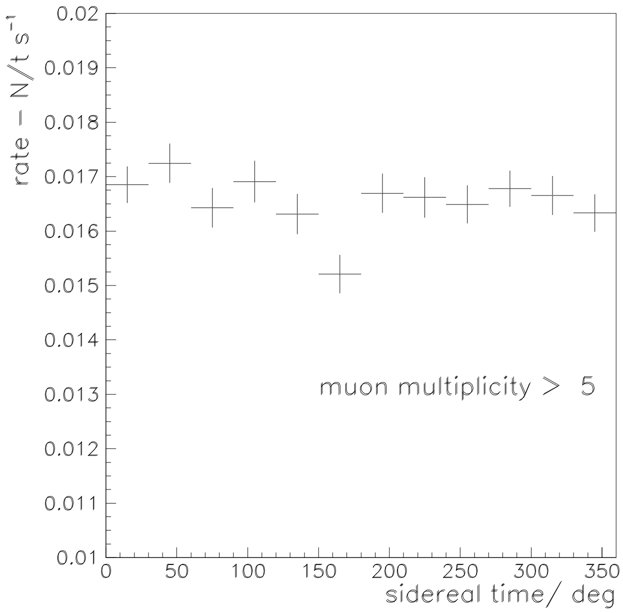

Figure 13: The event rate versus the sidereal time expressed in degrees. Events with more than 5 reconstructed muons are taken into account.

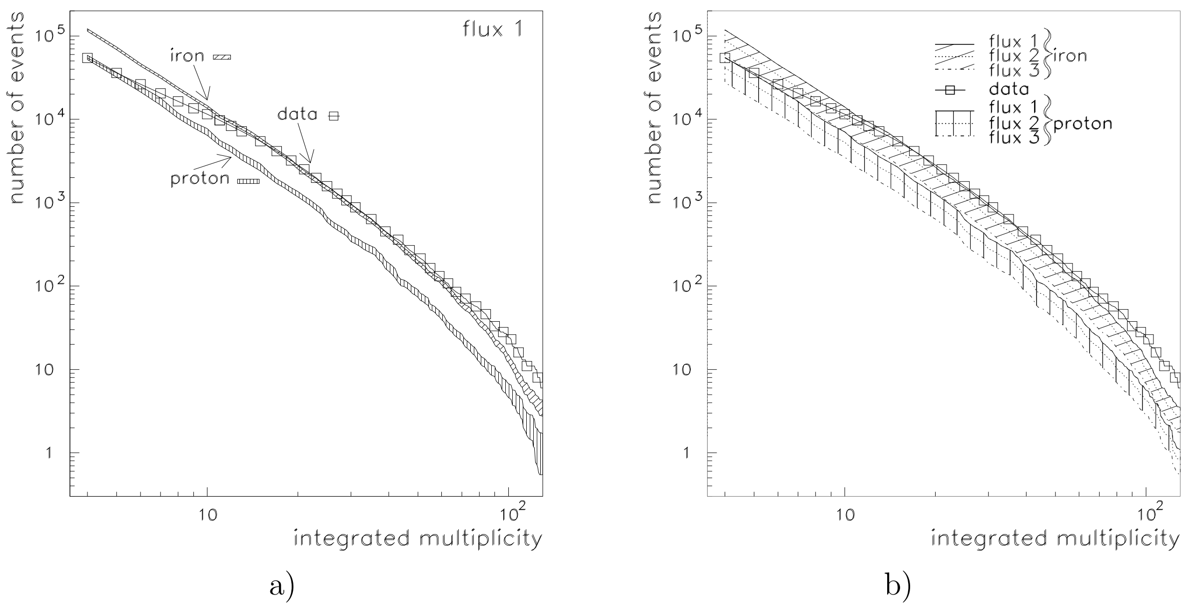

Figure 14: Integrated multiplicity measured in HAB together with the result of the MC simulation of iron and proton induced showers with assumed flux *1* (a) and fluxes *1 - 3* (b).

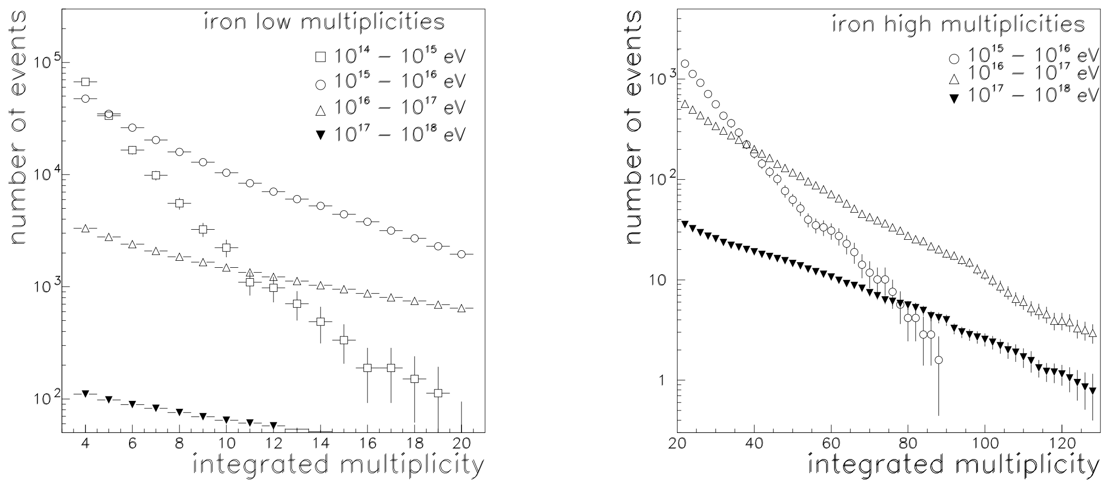

Figure 15: Contributions of different energy intervals to the final integral multiplicity distribution. Primary particles are iron nuclei.

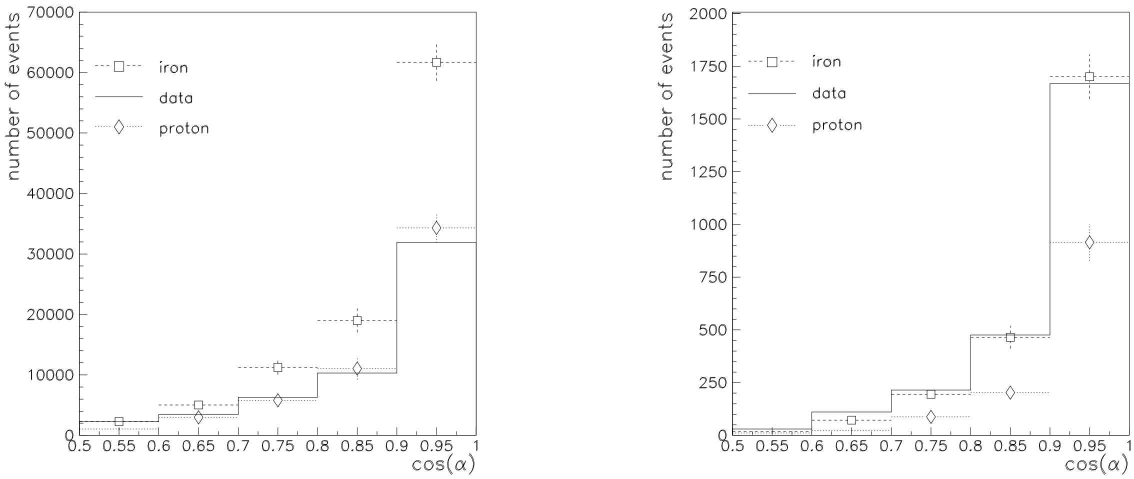

a) b)

Figure 16: Cosine of the projected angle α at $N_\mu \geq 4$ (a) and $N_\mu \geq 20$ (b) for iron simulation (squares), data (full line) and proton simulation (diamonds). Normalisation of MC curves is done according to flux 1 from Fig. 11.

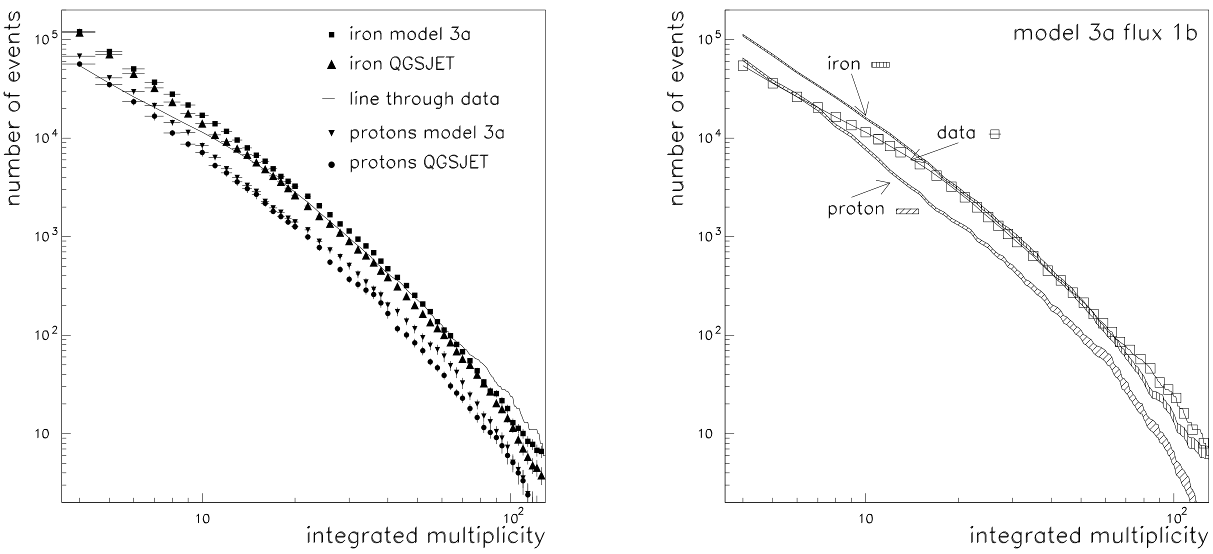

a) b)

Figure 17: (a) The integral multiplicity distribution for QGSJET and modification *3a* compared to data. Flux *1* is assumed. (b) The integral multiplicity distribution for the modification *3a* compared to data. Flux *1b* is assumed.